

Chiral recognition of dipeptides in phosphatidylcholine aggregates

Oscar Cruciani,^{a,b} Stefano Borocci,^c Raffaele Lamanna,^d Giovanna Mancini^{a,b,e,*}
and Anna Laura Segre^a

^a*Istituto di Metodologie Chimiche-IMC, C.N.R., Area della Ricerca di Roma. C.P. 10, 00016 Monterotondo Stazione Roma, Italy*

^b*Dipartimento di Chimica, Università degli Studi di Roma 'La Sapienza', P.le A. Moro 5, 00185 Roma, Italy*

^c*Dipartimento di Scienze Ambientali, Università degli Studi della Tuscia, P.le dell'Università, 01100 Viterbo, Italy*

^d*CR ENEA Trisaia UTS Biotec-Agro SS 106 Jonica Km 419.5, 75026 Rotondella (Mt), Italy*

^e*Centro di Eccellenza Materiali Innovativi Nanostrutturati per Applicazioni Chimiche Fisiche e Biomediche, Italy*

Received 24 June 2006; revised 12 September 2006; accepted 17 October 2006

Abstract—Enantiodiscrimination of ditryptophan enantiomers (L-Trp-L-Trp and D-Trp-D-Trp, L-Trp-D-Trp and D-Trp-L-Trp) was observed in bio-membrane models, such as micellar aggregates of 1,2-diheptanoyl-*sn*-glycero-3-phosphatidylcholine (DHPC) and multi-lamellar vesicles of either 1-palmitoyl-2-oleoyl-*sn*-glycero-3-phosphocholine (POPC) or 1,2-dimyristoyl-*sn*-glycero-3-phosphatidylcholine (DMPC) by solution ¹H NMR and HR-MAS ¹H NMR, respectively. The attainment of resolved signals, allowed the first detection of enantiodiscrimination at a molecular level, and the identification of the site of chiral recognition and of the interactions and conformations of homo- and heterochiral dipeptides in large-sized aggregates formed by a common component of bio-membranes.

© 2006 Elsevier Ltd. All rights reserved.

1. Introduction

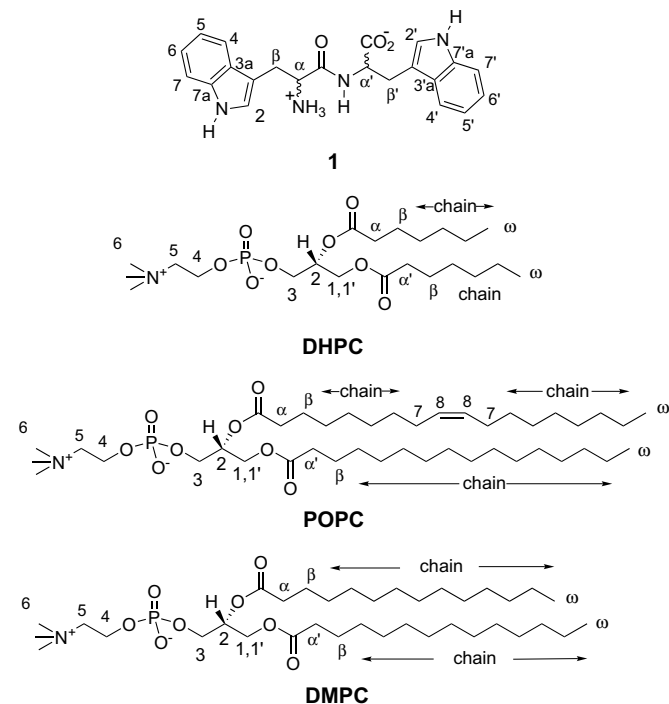
The process of lipid self-assembly to form biological membranes is at the basis of life. The lipid double layer, in fact, has not only the role of the protective barrier of the cell, because the organization of lipid molecules into the membrane double layer brings into being a large number of new functions that are fundamental to cell life and that are not operative, though codified, in the single lipid entity. The functions of a bio-membrane are the result of a complex texture of molecular recognition processes, according to which, single molecules organize themselves into the lipid double layer, following patterns codified in their molecular structure. Since most membrane components are chiral and enantiopure, chirality is a part of the program codified in the molecular structure and influences the membrane organization and functions by way of enantiospecific interactions.

Several studies have been carried out on model systems for investigating the role of chirality in the organization and function of bio-membranes;^{1–19} however, it has not yet been clarified how and where exactly the chiral function is transferred from the molecule to the lipid assembly and how it is expressed in the complex biological membrane system. Investigations aimed at clarifying the expression of enantiospecific lipid–lipid interactions revealed that homochiral aggregates are characterized by different physical–chemical features with respect to aggregates formed by racemic mixtures,^{1–5} whereas the expression of the chiral function of model membrane aggregates into recognition properties towards other chiral molecules was detected in only a few cases.^{7–10} Interestingly the investigations on enantiodiscrimination in aggregates formed by phosphatidylcholines gave contrasting results. In fact, the chiral recognition of odorants in DPPC monolayers,¹¹ the deracemization of a helical-shaped molecule in DPPC vesicles,^{12,13} and the requirement of a specific chirality of membrane lipids for peptide-induced formation of cholesterol-rich domains¹⁷ were reported. On the other hand, investigations aimed at verifying whether, and to what extent lipid bilayers can assist the polycondensation of amino acids, did not give any evidence of discrimination between enantiomers;⁶ analogously, no enantioselective

* Corresponding author at present address: CNR, Istituto di Metodologie Chimiche, Dipartimento di Chimica 'La Sapienza', P.le A. Moro 5, Roma 00185, Italy. Tel.: +39 0649913078; fax: +39 06490421; e-mail: giovanna.mancini@uniroma1.it

interaction was shown to be involved in the nicotinic acetylcholine receptor sterol activation site,¹⁸ and in the inhibition of mechanosensitive channels by neuroactive peptides.¹⁹

The aim of this investigation was to explore the capability of phosphatidylcholine aggregates to discriminate enantiomeric molecules and to investigate how changes in the structure of the hydrophobic residue of the monomer, and therefore in the morphology of the aggregates, influence chiral discrimination in membrane models. With this in mind, we investigated the ¹H NMR of the four stereoisomers of ditryptophan **1** (LL-**1** and DD-**1**, LD-**1** and DL-**1**) in micellar aggregates formed by 1,2-diheptanoyl-*sn*-glycero-3-phosphatidylcholine, DHPC, and in multilamellar vesicles (MLV) formed by either 1-palmitoyl-2-oleoyl-*sn*-glycero-3-phosphocholine, POPC, or 1,2-dimyristoyl-*sn*-glycero-3-phosphatidylcholine, DMPC. Micellar aggregates were investigated by static ¹H NMR, whereas multilamellar vesicles were investigated under magic angle conditions, namely HR-MAS.



Herein we report the observation of the enantiodiscrimination of LL-**1**/DD-**1** and LD-**1**/DL-**1** enantiomer couples in all the aggregates investigated. NMR investigations allowed us to detect also the site of recognition and, combined with Molecular Mechanics calculations, the conformations of dipeptides inside the aggregates.

2. Results and discussion

The dipeptide/aggregate interactions and the conformation of the dipeptides in the aggregates (micelles of DHPC, multilamellar dispersions of POPC and DMPC), have been investigated by 1D and 2D NMR experiments performed

at 600.13 MHz. Experiments concerning multilamellar dispersions of POPC and DMPC have been performed under HR-MAS conditions.

The aromatic region of the ¹H NMR spectra of the enantiomer couples of **1** (i.e., LL-**1**/DD-**1** and LD-**1**/DL-**1**) 5 mM in a D₂O solution of 50 mM DHPC (in 100 mM phosphate buffer, pD = 5.8) are reported in Figures 1 and 2, whereas the same region of the spectra relative to the experiments performed in the presence of multilamellar dispersion of DMPC and POPC at [lipid]/[peptide] = 10 (100 mM phosphate buffer, pD = 5.8) are reported in Figures 3–6, respectively. The complete assignment of the resonances due to the ditryptophan reported in Figures 1–6 has been performed as reported previously.⁹

It can be observed that the NMR spectra of the enantiomers, in the presence of aggregates (either micelles or vesicles), formed by phosphocholines are different. Diastereomeric interactions between chiral aggregates and peptides yield different chemical shifts for some of the resonances of the enantiomers of **1**. In Table 1 we report ¹H chemical shift differences of the resonances of homo-chiral (DD resonances subtracted from LL resonances) and heterochiral (DL resonances subtracted from LD resonances) couples of **1** in the presence of different aggregates.

In analogous investigations carried out in the presence of micellar aggregates formed by a proline derivative we observed a discrimination of the enantiomers of **1** and of

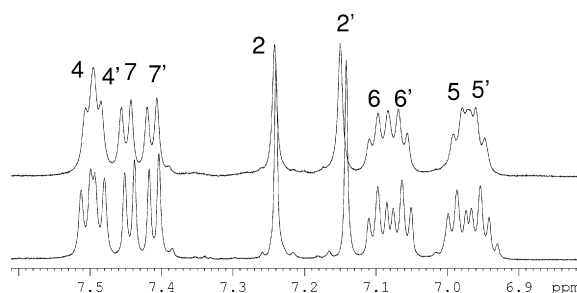


Figure 1. Comparison of the aromatic region of the 600.13 MHz ¹H NMR spectra of 5 mM **1** homochiral enantiomers in 50 mM DHPC (DD-**1** top, LL-**1** down). The spectra were obtained in an aqueous buffered solution (100 mM phosphate buffer, pD = 5.8) at 300 K.

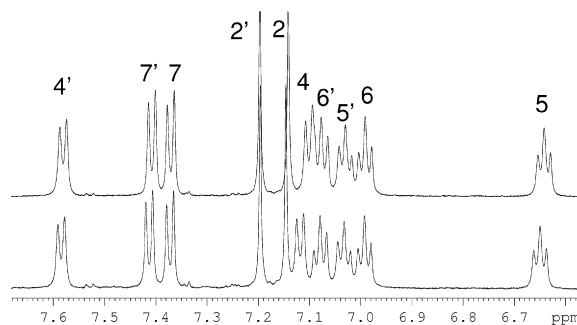


Figure 2. Comparison of the aromatic region of the 600.13 MHz ¹H NMR spectra of 5 mM **1** heterochiral enantiomers in 50 mM DHPC (LD-**1** top, DL-**1** down). The spectra were obtained in an aqueous buffered solution (100 mM phosphate buffer, pD = 5.8) at 300 K.

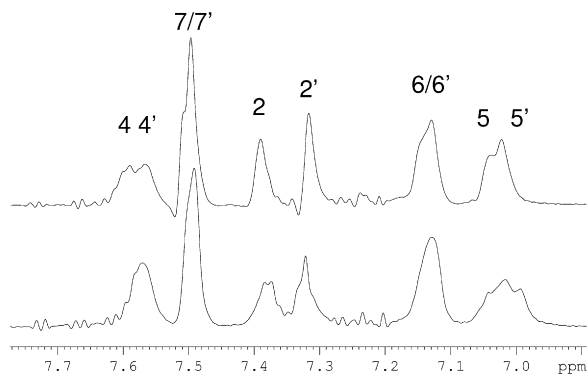


Figure 3. Comparison of the aromatic region of the 600.13 MHz ^1H HR-MAS spectra of 36 mM **1** homochiral enantiomers in the aqueous multilamellar dispersion of POPC (LL-1 top, DD-1 down). The spectra were obtained in an aqueous buffered solution (100 mM phosphate buffer, pD = 5.8) and performed at 10 kHz, setting the temperature at 300 K.

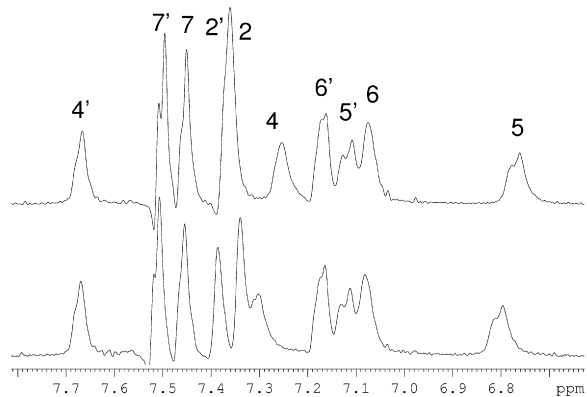


Figure 4. Comparison of the aromatic region of the 600.13 MHz ^1H HR-MAS spectra of 36 mM **1** heterochiral enantiomers in the aqueous multilamellar dispersion of POPC (LD-1 top, DL-1 down). The spectra were obtained in an aqueous buffered solution (100 mM phosphate buffer, pD = 5.8) and performed at 10 kHz, setting the temperature at 300 K.

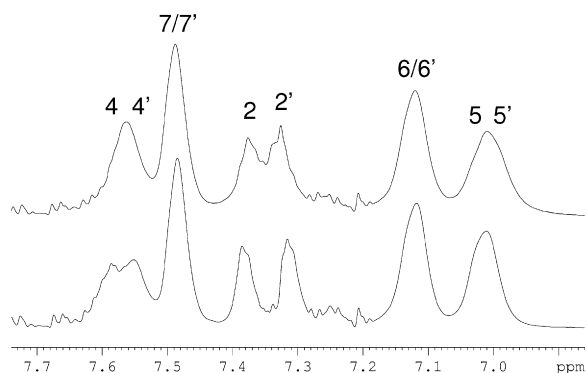


Figure 5. Comparison of the aromatic region of the 600.13 MHz ^1H HR-MAS spectra of 36 mM **1** homochiral enantiomers in the aqueous multilamellar dispersion of DMPC (LL-1 down, DD-1 top). The spectra were obtained in an aqueous buffered solution (100 mM phosphate buffer, pD = 5.8) and performed at 10 kHz, setting the temperature at 300 K.

other chiral molecules.^{9,15,16} However, this is the first time that enantiodiscrimination of biomolecules has been observed by NMR, that is, at a molecular level, in mem-

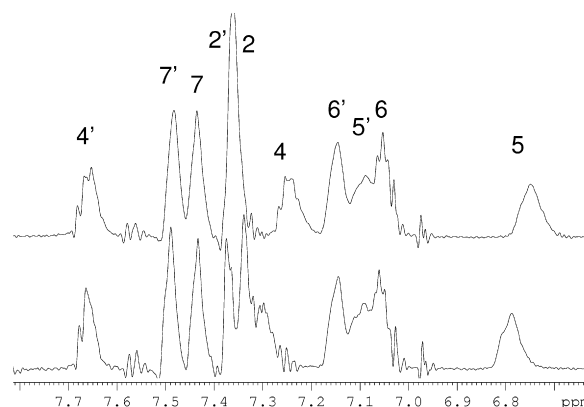


Figure 6. Comparison of the aromatic region of the 600.13 MHz ^1H HR-MAS spectra of 36 mM **1** heterochiral enantiomers in aqueous multilamellar dispersion of DMPC (LD-1 top, DL-1 down). The spectra were obtained in an aqueous buffered solution (100 mM phosphate buffer, pD = 5.8) and performed at 10 kHz, setting the temperature at 300 K.

Table 1. Chemical shift differences (Δ , in Hz) for the homochiral and heterochiral couples of **1** in the lipid aggregates

Type	Δ (Hz)					
	Micelles of DHPC		MLVs of POPC		MLVs of DMPC	
	LL/DD	LD/DL	LL/DD	LD/DL	LL/DD	LD/DL
α	0	-2	12	-6	12	-18
β	6	6	18	0	—	—
β	1	—	—	—	—	—
2	-1	-3	6	12	0	12
4	7	-10	24	-24	18	-30
5	5	-6	6	-18	0	-24
6	8	-2	6	0	0	-6
7	-3	-1	6	0	0	6
α'	-2	-1	-6	-6	-12	-12
β'	-10	8	-6	0	-18	-12
β'	-5	0	-6	18	—	0
2'	-5	1	0	-18	-12	-12
4'	-7	-2	6	0	-6	0
5'	-5	-2	24	0	12	0
6'	-4	-4	6	0	0	0
7'	-2	-4	6	-6	0	-6

brane models formed by phosphatidylcholines. Moreover, the use of HR MAS NMR,²⁰ by yielding sufficiently resolved spectra of semisolid samples, allowed us to observe enantiodiscrimination in models morphologically and thermodynamically similar to biological membranes.

It is worthy of note that the same couple of enantiomers were discriminated differently in the different aggregates. The DD-1/LL-1 couple is discriminated by the resonances of protons at positions β'_1 , 6 and 4 in DHPC micelles, by the resonances of protons at positions 4, 5' and β'_1 in the multilamellar dispersion of DMPC, and by the resonances of protons at positions 4, 5' and β in the multilamellar dispersion of POPC. The DL-1/LD-1 couple is discriminated by the resonances of protons in position β'_1 and 4 in DHPC micelles, by the resonances of protons at positions α , 4 and 5 in multilamellar dispersion of DMPC, and the resonances of protons at positions β'_2 , 2', 4 and 5 in the multilamellar dispersion of POPC.

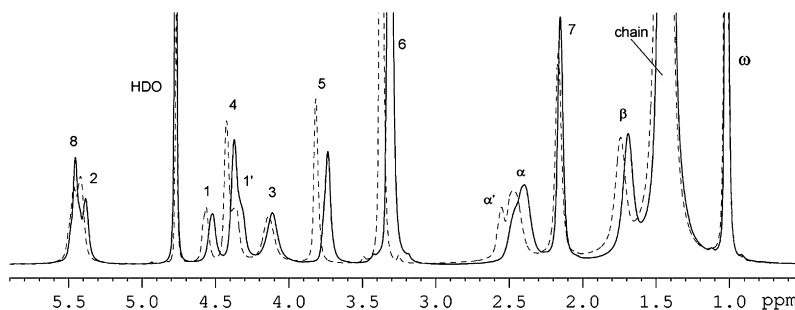


Figure 7. Comparison of the 600.13 MHz ^1H HR-MAS NMR (10 kHz) spectra of the aqueous multilamellar dispersion of POPC in the absence (grey dashed trace) and in the presence of DD-1 (black trace).

The effect of the aromatic systems of **1** on the chemical shift of resonances due to lipids was also investigated, because it gives information on the site of binding of the stereoisomers of **1**. In Figure 7 the comparison of the NMR spectrum of an aqueous multilamellar dispersion of POPC in the presence and in the absence of one of **1** stereoisomers (DD-1) with a complete spectral assignment can be seen. The chemical shift differences (expressed in hertz) observed for each aggregate model between the spectra performed in the absence and in the presence of dipeptides are reported in Table 2. All resonances due to phosphocholine protons are upfield shifted; however, the shift is more relevant for the protons of the upper acyl chain segments near to the glycerol backbone (α , α' and β) and for the protons of the choline residue (6, 5 and 4) indicating that these protons lie preferentially within the shielding cone of the aromatic system²¹ and suggesting the headgroup region as the preferential location of all the stereoisomers of **1** in all the model aggregates.

All the stereoisomers have a similar position inside the aggregate independent of the different curvature of micelles and vesicles and independent of the organization of the aggregates due to the different nature of the hydrophobic residue. The relevant chemical shift variation observed for the signal relative to choline residue protons suggests, in the balance of all interactions involved, an important role of a cation– π interaction between the ammonium group and the aromatic systems of the dipeptides. The

extent of the variation of the chemical shift of the first segment of the hydrophobic chain (protons at the α - and β -positions) and the smaller effect on the protons at the 2- and 3-positions confirm the previously suggested folding of the choline residue toward the interior of the aggregates that yields the negative-charged surface detected by capillary electrophoresis experiments.²² A minor involvement of the hydrophobic region, as the site of binding, with respect to the head group region is indeed suggested by the extent of the shift of DHPC aliphatic chain signals (chain and ω ; note that in this case, the chain signal is due only to three methylene protons) and of POPC olefinic protons (7 and 8). The similar trend observed for all the analogous signals of DMPC suggests similar situations in the aggregates formed by this lipid. These results also are in agreement with a previously reported interfacial location of analogues of tryptophan in aggregates formed by POPC.²³

Although the location is the same in all the model aggregates investigated, the values of chemical shift difference reported in Table 2 show that the same stereoisomer features in each model different interactions. For example, in the columns relative to LL-1 (Table 2), if we consider the values relative to the α , α' and β protons, we see that a signal due to the α -proton of POPC features the same chemical shift variation of the signal due to the α' -proton and a higher chemical shift variation with respect to the β -proton, whereas the trend is different in DMPC

Table 2. Chemical shift variations of the signals due to the aggregates in the presence of dipeptides

Type	LL-1			DD-1			DL-1			LD-1		
	POPC	DMPC	DHPC	POPC	DMPC	DHPC	POPC	DMPC	DHPC	POPC	DMPC	DHPC
ωCH_3	6	0	10	6	0	11	0	0	13	0	0	13
Chain	6	6	19	6	6	17	6	6	20	6	6	20
α	42	36	28	36	30	28	24	30	27	30	30	26
α'	42	48	26	54	54	26	36	54	27	42	48	28
β	30	30	25	24	24	24	24	24	24	24	24	24
1	18	18	15	18	24	16	12	12	11	12	12	10
1'	24	18	14	30	12	13	12	12	8	12	12	9
2	18	18	9	18	12	10	6	6	4	6	6	4
3	12	18	8	12	12	8	0	6	3	0	6	2
4	30	24	25	36	24	25	24	18	19	24	18	19
5	48	42	41	54	42	41	36	36	35	36	36	35
6	36	36	30	42	30	29	30	30	26	30	30	26
7	12	—	—	12	—	—	12	—	—	6	—	—
8	6	—	—	12	—	—	6	—	—	6	—	—

Table 3. Interproton distances (Å) obtained by NOESY and ROESY experiments and used as restraints in molecular mechanics calculations

	DHPC buffered solution ^a				POPC buffered solution ^b				DMPC buffered solution ^b			
	LL-1	DD-1	LD-1	DL-1	LL-1	DD-1	LD-1	DL-1	LL-1	DD-1	LD-1	DL-1
β -4	—	—	2.8 ^c	2.5 ^c	—	—	3.0	—	2.7	—	3.0	—
β' -4'	3.1	3.2	3.1 ^d	3.1 ^d	3.1 ^c	3.1 ^c	3.1 ^d	3.1 ^d	3.3 ^c	3.2 ^c	3.2 ^d	2.9 ^d
α -4	2.8	2.7	2.8	2.7	2.7	2.7	3.0	2.8	2.8	2.9	3.3	2.7
α' -4'	3.0	3.1	2.9	2.9	3.1	3.2	2.9	3.0	3.3	3.5	2.9	2.8

^a ROESY experiments (5 mM dipeptide and 50 mM DHPC in 100 mM phosphate buffer).

^b NOESY experiments (36 mM dipeptide and 362 mM POPC in 100 mM phosphate buffer).

^c Signals due to diastereotopic β (β') protons are coincident.

^d The distance reported is the average of the distances obtained for the diastereotopic β' protons ($\langle r \rangle = \langle r^6 \rangle^{1/6}$; $(1/r^6 + 1/r'^6)/2 = 1/\langle r^6 \rangle$).

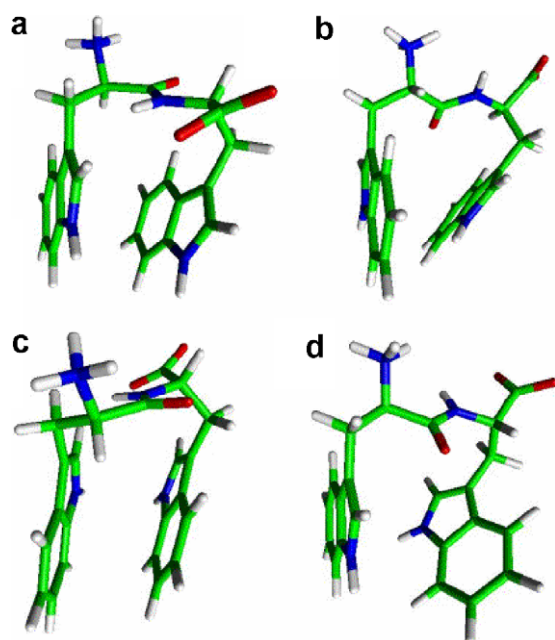


Figure 8. Stick representation of the minimum energy conformer, obtained by a restrained conformational search, of (a) DD-1 in POPC, (b) LD-1 in POPC, (c) LL-1 in POPC, (d) DL-1 in POPC.

($\alpha' > \alpha > \beta$) and DHPC ($\alpha \approx \alpha' \approx \beta$). Similar observations can be done for the other stereoisomers (e.g., β , 1 and 1' for DD-1 and α , α' and β for heterochiral dipeptides). This shows that although the three lipids feature the same chiral headgroup, the interactions of the solutes with the headgroups in the aggregates formed by each lipid are different. This observation, and the fact that each couple of enantiomers is discriminated differently in the different aggregates (Table 1), supports the hypothesis that chiral recognition in polymolecular aggregates is due to a whole region of the aggregate rather than to the interaction with the stereogenic center of a single monomer and, therefore that the chiral information is translated from the monomer to the aggregate through a complex mixture of interactions.

In order to investigate the conformation of the four stereoisomers of **1** associated with the phosphocholine aggregates, we carried out a conformational search by means of molecular mechanics calculations using, as distance restraints, the experimental distances (Table 3) obtained by ROESY (micellar aggregates of DHPC) and by NOESY (vesicular aggregates of POPC and DMPC) experiments.

The conformations obtained are substantially similar in DHPC micelles and POPC or DMPC vesicles. As an exam-

Table 4. Torsional angles of low energy conformers of ditryptophan stereoisomers, in the different aggregates, obtained by molecular mechanics calculations

Dipeptide	ψ	ϕ	ω	χ_1	χ_2	χ'_1	χ'_2
<i>Dipeptides in DHPC micelles</i>							
LL-1	-115.2	-169.1	-179.7	-168.4	-111.8	-71.2	79.9
DD-1	115.2	169.0	179.6	168.4	111.8	71.1	-79.9
LD-1	65.7	146.6	178.9	-179.9	-118.9	173.8	-111.7
DL-1	-65.7	-146.7	-178.8	179.9	118.8	-173.8	111.7
<i>Dipeptides in POPC MLVs</i>							
LL-1	-115.2	-169.1	-179.6	-168.4	-111.8	-71.2	80.0
DD-1	115.4	169.0	179.7	168.4	111.8	-71.2	-79.9
LD-1	65.6	146.7	178.8	-179.9	-118.9	173.7	-111.7
DL-1	-65.6	-146.7	-178.8	179.9	118.9	-173.7	111.8
<i>Dipeptides in DMPC MLVs</i>							
LL-1	-115.2	-169.1	-179.7	-168.4	-111.8	-71.2	79.9
DD-1	115.2	169.1	179.7	168.4	111.8	71.1	-79.9
LD-1	65.6	146.7	178.8	-179.9	-118.8	173.7	-111.7
DL-1	-65.6	-146.6	-178.8	179.9	118.9	-173.8	111.8

$\psi = \text{H}_3\text{N}^+-\text{C}^\alpha-\text{C}(\text{O})-\text{NH}$; $\phi = \text{C}(\text{O})-\text{NH}-\text{C}^\beta-\text{CO}_2^-$; $\omega = \text{O}-\text{C}(\text{O})-\text{N}-\text{H}$; $\chi_1 = \text{H}_3\text{N}^+-\text{C}^\alpha-\text{C}^\beta-\text{C}^3$; $\chi_2 = \text{C}^\alpha-\text{C}^\beta-\text{C}^3-\text{C}^2$; $\chi'_1 = \text{HN}-\text{C}^\alpha-\text{C}^\beta-\text{C}^3$; $\chi'_2 = \text{C}^\alpha-\text{C}^\beta-\text{C}^3-\text{C}^2$.

ple, the conformations of the diastereoisomers of **1** relative to the experiments in POPC vesicles are reported in Figure 8, whereas the torsion angles relative to the structures defined by an energy minimum are given in Table 4 for all experiments. The conformation of homochiral dipeptides (Fig. 8a and c) is ‘folded’: the aromatic portions of the amino acid residues face each other in an almost mirror-like mode. The conformation of heterochiral dipeptides (Fig. 8b and d), is completely different, as the planes of the aromatic residues are not parallel and the indolic residues are oriented differently so that nitrogen atoms point towards opposite directions. The specific interactions with the aggregates impose different conformations to homo- and heterochiral ditryptophan; these conformations are different with respect to those found in phosphate buffer (previously reported⁹), similar for both homo- and heterochiral ditryptophan, folded and with indolic residues oriented in opposite directions.

3. Conclusions

We have observed, by ¹H NMR, the chiral recognition of the enantiomer couples of ditryptophan in micelles and vesicles formed by phosphatidylcholines. To the best of our knowledge, this is the first time that the enantio-discrimination of biomolecules has been observed by NMR, that is, at a molecular level, in a membrane model formed by phosphatidylcholines. 1D NMR experiments also suggested that the association site of all stereoisomers is in the headgroup region, in all the models investigated, independently on the surface curvature and on the organization of the aggregates. However, the morphology and/or the organization of each model affects the specificity of recognition and of interaction with the dipeptides. This is in agreement with the recent findings of a different extent of deracemization of a helical-shaped molecule as a function of the size, and therefore, of the different curvature and organization of different-sized phosphatidylcholine vesicles.¹³

The different conformations of homo- and heterochiral enantiomers obtained by bidimensional NOE experiments combined with Molecular Mechanics Calculations, though substantially similar in all the models investigated, are the results of specific interactions with different aggregates.

The finding of enantiodiscrimination in membrane models formed by the components of natural membranes supports the view that chirality plays a fundamental role in the organization of biological membranes. A full understanding of chiral expressions in bio-membranes will not only clarify important aspects of the function of these systems, but it will also have implications in the understanding of the transfer of chirality from the molecular to higher organization levels. Furthermore, it will open up new perspectives in considering a possible role of these biological systems in the history of the lack of chiral symmetry of Nature, especially in amplification processes of an initially small enantiomeric imbalance yielded by any of the possible physiochemical processes proposed.^{24–26}

4. Experimental

4.1. Materials

1,2-Diheptanoyl-*sn*-glycero-3-phosphatidylcholine (DHPC), 1-palmitoyl-2-oleoyl-*sn*-glycero-3-phosphatidylcholine (POPC) and 1,2-dimyristoyl-*sn*-glycero-3-phosphatidylcholine (DMPC) were purchased from Avanti Polar Lipids (Alabaster, AL, USA) and used without further purification. The LL/DD enantiomer couple of ditryptophan **1** were purchased from Research Plus Inc. and used as such. The other two isomers of **1**, LD-**1** and DL-**1**, were prepared as previously described.⁹ D₂O (99.9% atom D) was purchased from Cambridge Isotope Laboratories, Inc. All other reagents of the highest purity grade were from Fluka or Sigma-Aldrich.

4.2. Samples

A 100 mM sodium phosphate buffer in D₂O was used to prepare all solutions considered in this investigation (pD = 5.8). DHPC micellar samples were prepared 50 mM (well above the 1.9 mM critical micellar concentration²⁷).

The solutions of dipeptides were prepared by directly dissolving into the NMR sample tubes 1.4 mg of **1** in 700 μ L (5 mM) of micellar solution.

The samples of POPC, POPC/peptide (in a 10:1 molar ratio), DMPC and DMPC/peptide (in a 10:1 molar ratio) were prepared by dissolving the proper amount of lipid and, when necessary, of **1** in CHCl₃. The samples were vortex mixed and the organic solvent was removed by roto-evaporation followed by high-vacuum pumping overnight. The samples were then hydrated using a 100 mM sodium phosphate buffer in D₂O to obtain a final concentration of POPC or DMPC = 362 mM and were taken through five cycles of vortex mixing and freeze-thawing to obtain homogeneous dispersions.

4.3. NMR experiments

1D and 2D NMR experiments were performed on a Bruker AVANCE AQS600 spectrometer operating at 600.13 MHz and 150 MHz for the ¹H and ¹³C Larmor frequency, respectively. The spectrometer was equipped with a Bruker multinuclear inverse probe head. ¹H NMR spectra were referenced with respect to the residual proton signal of D₂O (δ = 4.780 ppm at 300 K). All 1D experiments were performed without suppression of the residual HDO signal. The spectral assignment was performed using conventional 2D experiments,²⁸ as reported previously.⁹

ROESY (rotating frame Overhauser enhancement spectroscopy)²⁸ experiments were performed in the TPPI phase sensitive mode with a spectral sweep width of 6 kHz in both dimensions, 1024 data points in f_2 and 512 increments in f_1 , and a recycle delay of 2 s. A mixing time of 80 ms was used, and mixing was achieved by the continuous wave method with a field strength of 5 kHz. Zero filling in f_1 to 1024 real data points and 90° phase-shifted square-sine bell window functions in both dimensions were applied

before Fourier transformation. All HR-MAS experiments were performed on a Bruker AVANCE 600 spectrometer operating at 600.13 MHz, using a Bruker HR-MAS probe with an internal lock. The samples were loaded in 4 mm ZrO₂ cylindrical rotors with spherical inserts (internal volume of 45 μ L). All HR-MAS NMR experiments were performed setting the temperature at 300 K and with a spinning speed of 10 kHz, accumulating 256 or 1K FIDs with 16K data points (time domain) and a spectral width of 6.5 kHz. A 90° excitation pulse (7–8 μ s) was used with a relaxation delay of 2 s. Prior to Fourier transformation, the data were zero filled to 16K points and resolution enhanced using a Gaussian multiplication (LB = –14 Hz, GB = 0.1245 Hz) or apodized using an exponential line broadening of 1 Hz. The spectral assignment was performed with the usual 2D techniques.²⁸ All the 2D experiments in HR-MAS condition were performed setting the temperature at 300.0 K and with a spinning speed of 10 kHz.

2D-NOESY²⁸ spectra were obtained in TPPI phase-sensitive mode, using a spectral width of 6 kHz width in both dimensions, 512 increments, 32 scans, 1K data points, a relaxation delay of 2 s and mixing times of 10 ms. Sine squared window functions in both dimensions were applied before Fourier transformation.

All the experiments were performed after a sufficient equilibration time.

4.4. Determination of the dipeptide intramolecular distances

Inter-proton distances were obtained by integration of the cross-peaks in ROESY/NOESY spectra as previously described in an analogous investigation.⁹

4.5. Molecular modelling

Molecular mechanics calculations were performed with the MacroModel 6.0 package²⁹ running on a Silicon Graphics O2 R10000 workstation, and using AMBER* force field. The electrostatic interactions were evaluated using the partial atomic charges of the AMBER* force field;^{30,31} a dielectric constant of 10 was used to reproduce the micellar^{32,33} medium. A conformational search with distance restraints was carried out on the molecular structures of the four stereoisomers of ditryptophan as described previously.⁹

Acknowledgements

This work has been carried out in the frame of the project ‘The use of surfaces and vesicles for the amplification of homochirality in polypeptide chains’ of COST action D27. We acknowledge contributions from CNR, Dipartimento di Progettazione Molecolare.

References

- Arnett, E. M.; Thompson, O. *J. Am. Chem. Soc.* **1981**, *103*, 968–970.
- Arnett, E. M.; Gold, J. M. *J. Am. Chem. Soc.* **1982**, *104*, 636–639.
- Fuhrhop, J. H.; Schnieder, P.; Rosenberg, J.; Boekema, E. *J. Am. Chem. Soc.* **1987**, *109*, 3387–3390.
- Morigaki, K.; Dallavalle, S.; Walde, P.; Colonna, S.; Luisi, P. L. *J. Am. Chem. Soc.* **1997**, *119*, 292–301.
- Uragami, M.; Miyake, Y.; Regen, S. L. *Langmuir* **2000**, *16*, 3491–3496.
- Hitz, T.; Luisi, P. L. *Biopolymers* **2000**, *55*, 381–390.
- Lalitha, S.; Kumar, A. S.; Stine, K. J.; Covey, D. F. *J. Supramol. Chem.* **2001**, *1*, 53–61.
- Borocci, S.; Ceccacci, F.; Galantini, L.; Mancini, G.; Monti, D.; Scipioni, A.; Venanzi, M. *Chirality* **2003**, *15*, 441–447.
- Bombelli, C.; Borocci, S.; Lupi, F.; Mancini, G.; Mannina, L.; Segre, A. L.; Viel, S. *J. Am. Chem. Soc.* **2004**, *126*, 13354–13362.
- Mohanty, A.; Dey, J. *J. Chromatogr. A* **2005**, *1070*, 185–192.
- Pathirana, S.; Neely, W. C.; Myers, L. J.; Vodyanoy, V. *J. Am. Chem. Soc.* **1992**, *114*, 1404–1405.
- Nakagawa, H.; Yoshida, M.; Kobori, Yuuki; Yamada, K.-I. *Chirality* **2003**, *15*, 703–708.
- Nakagawa, H.; Onoda, M.; Masuoka, Y.; Yamada, K.-I. *Chirality* **2006**, *18*, 212–216.
- Walde, P.; Blöchliger, E. *Langmuir* **1997**, *13*, 1668–1671.
- Bella, J.; Borocci, S.; Mancini, G. *Langmuir* **1999**, *15*, 8025–8031.
- Andreani, R.; Bombelli, C.; Borocci, S.; Lah, J.; Mancini, G.; Mencarelli, P.; Vesnaver, G.; Villani, C. *Tetrahedron: Asymmetry* **2004**, *15*, 987–994.
- Epand, R. M.; Rychnovsky, S. D.; Belani, J. D.; Epand, R. F. *Biochem. J.* **2005**, *390*, 541–548.
- Addona, G. H.; Sandermann, H., Jr.; Kloczewiak, M. A.; Miller, K. W. *Biochim. Biophys. Acta* **2003**, *1609*, 177–182.
- Suchyna, T. M.; Tape, S. E.; Koeppel, R. E., II; Andersen, O. S.; Sachs, F.; Gottlieb, P. A. *Nature* **2004**, *430*, 235–240.
- Davis, J. H.; Auger, M. *Prog. Nucl. Magn. Reson. Spectrosc.* **1999**, *35*, 1–84.
- Haigh, C. W.; Mallion, R. B. *Prog. Nucl. Magn. Reson. Spectrosc.* **1980**, *13*, 303–344.
- Corradini, D.; Mancini, G.; Bello, C. *Chromatographia* **2004**, *60*, S125–S132.
- Yau, W.-M.; Wimley, W. C.; Gawrisch, K.; White, S. H. *Biochemistry* **1998**, *37*, 14713.
- Avalos, M.; Babiano, R.; Cintas, P.; Jiménez, J. L.; Palacios, J. C. *Tetrahedron: Asymmetry* **2000**, *11*, 2845–2874.
- Bonner, W. A. *Chem. Ind. (London)* **1992**, *17*, 640–644.
- Bailey, J. *Acta Astronaut.* **2000**, *46*, 627–631.
- Walde, P.; Blöchliger, E.; Morigali, K. *Langmuir* **1999**, *15*, 2346–2350.
- Braun, S.; Kalinowski, H.-O.; Berger, S. *150 and More Basic NMR Experiments. A Practical Course*; Wiley-VCH: Weinheim, Germany, 1998.
- Mohamadi, F.; Richards, N. G. J.; Guida, W. C.; Liskamp, R.; Lipton, M.; Caufield, C.; Chang, G.; Hendrikson, T.; Still, W. C. *J. Comput. Chem.* **1990**, *11*, 440–467.
- Weiner, S. J.; Kollman, P. A.; Case, D. A.; Singh, U. C.; Ghio, C.; Alagona, G.; Profeta, S., Jr.; Weiner, P. *J. Am. Chem. Soc.* **1984**, *106*, 765–784.
- McDonald, D. Q.; Still, W. C. *Tetrahedron Lett.* **1992**, *33*, 7747–7750.
- Bunton, C. A.; Minch, M. J.; Hildago, J.; Sepulveda, L. *J. Am. Chem. Soc.* **1973**, *95*, 3262–3272.
- Carpenter, K. A.; Wilkes, B. C.; Weltrowska, G.; Schiller, P. W. *Eur. J. Biochem.* **1996**, *241*, 756–764.